Chapter 11
Neural Network Modeling of Voluntary Single-Joint Movement Organization II. Parkinson's Disease

Vassilis Cutsuridis

Abstract The organization of voluntary movement is disrupted in Parkinson's disease. The neural network models of voluntary movement preparation and execution presented in the previous chapter are extended here by studying the effects of dopamine depletion in the output of the basal ganglia and in key neuronal types in the cortex and spinal cord. The resulting extended DA–VITE–FLETE model offers an integrative perspective on corticospinal control of Parkinsonian voluntary movement. The model accounts for most of the known empirical signatures of Parkinsonian willful action.

11.1 Introduction

Parkinson's disease (PD) is a disabling motor disorder that affects all kinds of movements. In the early stages of PD, patients have difficulty with walking, speaking, or getting in and out of chairs [33]. As the disease progresses, all movements are affected resulting at the end of the disease a complete inability to move. Patients require intense concentration to overcome the apparent inertia of the limbs that exists even for the simplest motor tasks. Movement initiation is particularly impaired when novel movements or sequences of movements are attempted [16, 3, 41].

The lack of understanding of the causes of PD and the problems associated with its treatment have led to the search for appropriate animal models. Over the years, two experimental methods have been employed to induce Parkinsonism in animals: (1) application of reserpine, alpha-methyl-p-tyrosine (AMPT) [14], and 1-methyl-4-phenyl-1,2,3,6-tetrahydropyridine (MPTP) [12] resulting in dopamine depletion in the brain and (2) stereotaxic lesions with focal injections of 6-hydroxydopamine

V. Cutsuridis
Centre for Memory and Brain, Boston University, Boston, MA, USA,
e-mail: vcut@bu.edu

W. Chaovalitwongse et al. (eds.), *Computational Neuroscience*,
Springer Optimization and Its Applications 38, DOI 10.1007/978-0-387-88630-5_11,

(6-OHDA) into the substantia nigra or medial forebrain bundle to destroy the ascending dopamine tracts. Depending on the method used, the effects vary and can be temporary or permanent.

MPTP administration in primates produces three distinct phases of altered motor activity: acute phase, subacute phase, and chronic phase [12]. In the acute phase after administration, animals appear to go to sleep and fall slowly from their perches to the floor of the cage; their eyes remain open, but with a vacant gaze [12]. Occasionally, wild running or exaggerated startle response events are observed [12]. The acute effects of MPTP last approximately 0.5–1.0 h and then disappear until subsequent administration [12].

During the subacute phase after MPTP administration, persistent motor deficits develop. Animals become increasingly akinetic and show rigidity of the limbs, freezing episodes, postural abnormalities, and loss of vocalization and blink reflex [12]. Compulsive climbing behavior can also occur at this stage, causing animals to damage their heads and faces [12]. This spectrum of behavioral effects lasts for some weeks, but the animals slowly recover. In subsequent weeks the motor deficits stabilize, and the animals enter the chronic phase of MPTP action. They show less spontaneous movements, although when challenged, they can move freely in the home cage [12]. Complex movements are poorly coordinated and clumsily executed. Hesitation prior to movement is apparent, and the range of movements observed appears limited [12].

Postmortem studies of PD in humans [22] and MPTP-treated rhesus monkeys [44] have shown that the toxin destroys the cells of the substantia nigra pars compacta, but not of the locus coereleus, dorsal raphe, and substantia nigra innominata [12]. Within the substantia nigra, the cells in the centrolateral area of the SNc are damaged more extensively than those in the medial portion of the SNc [32]. Administration of MPTP to young primates causes a profound ($> 90\%$) persistent loss of caudate-putamen dopamine content that is irreversible by any form of medication. The ventral tegmental area (VTA) adjacent to the substantia nigra shows limited and variable damage to tyrosine hydroxylase-containing cells in MPTP-induced Parkinsonism [12].

11.2 Brain Anatomy in Parkinson's Disease

The difficulty in understanding and treating Parkinson's disease is because there are multiple brain areas and pathways affected from the sites of neuronal degeneration all the way to the muscles. Figure 11.1 depicts three of these pathways: (1) the pathway from the substantia nigra pars compacta (SNc) and the ventral tegmental area (VTA) to the striatum and from there to the thalamic nuclei and the frontal cortex through the substantia nigra pars reticulata (SNr) and the globus pallidus internal segment (GPi), (2) the pathway from the SNc and the VTA to the striatum and from there to the brainstem through the SNr and GPi, and (3) the pathway from

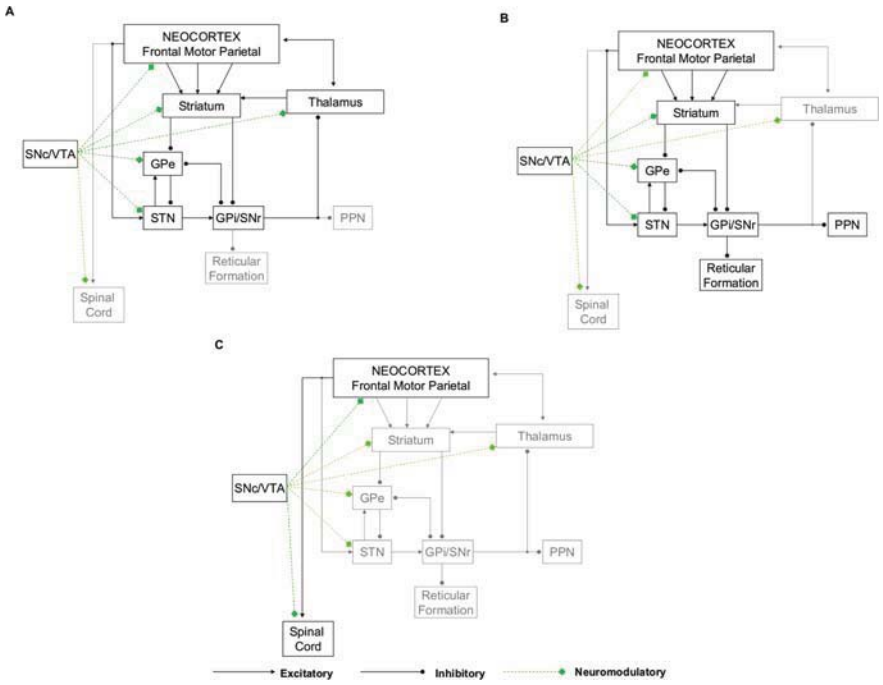

Fig. 11.1: Brain anatomical pathways in Parkinson's disease. (**A**) Pathways from the substantia nigra pars compacta (SNc) and the ventral tegmental area (VTA) to the striatum and from there to the thalamic nuclei and the frontal cortex through the substantia nigra pars reticulata (SNr) and the globus pallidus internal segment (GPi). (**B**) Pathway from the SNc and the VTA to the striatum and from there to the brainstem through the SNr and GPi. (**C**) Pathway from the SNc/VTA to cortical areas such as the supplementary motor area (SMA), the parietal cortex, and the primary motor cortex (M1), and from there to the spinal cord.

the SNc/VTA to cortical areas such as the supplementary motor area (SMA), the parietal cortex, and the primary motor cortex (M1), and from there to the spinal cord.

The most popular view is that cortical motor centers are inadequately activated by excitatory circuits passing through the basal ganglia (BG) [1]. As a result, inadequate facilitation is provided to the otherwise normally functioning motor cortical and spinal cord neuronal pools and hence movements are small and weak [1]. Recently, a new view has been introduced by the modeling studies of Cutsuridis and Perantonis [21] and Cutsuridis [18, 19, 20]. According to this view, the observed delayed movement initiation and execution in PD is due to altered activity of motor cortical and spinal cord centers because of disruptions to their input from the basal ganglia structures and to their dopamine (DA) modulation. The main hypothesis is that depletion of DA modulation from the SNc disrupts, via several pathways,

the buildup of the pattern of movement-related responses in the primary motor and parietal cortex and results in a loss of directional specificity of reciprocal and bidirectional cells in the motor cortex as well as in a reduction in their activities and their rates of change. These changes result in delays in recruiting the appropriate level of muscle force sufficiently fast and in an inappropriate scaling of the dynamic muscle force to the movement parameters. A repetitive triphasic pattern of muscle activation is sometimes needed to complete the movement. All of these disruptions result in an increase of mean reaction time and a slowness of movement.

11.3 Empirical Signatures

The validity of the model's hypothesis is based on the existence of a widespread dopaminergic innervation in not only the basal ganglia, but also in cortex and spinal cord as well as on its effects on movement, muscular, and neuronal parameters of Parkinson's disease patients and MPTP-lesioned animals.

11.4 Is There Dopaminergic Innervation of the Cortex and Spinal Cord?

A widespread dopaminergic innervation from the substantia nigra (SN), the VTA, and the retrorubral area (RRA) to the cortex and spinal cord exists [6, 54]. A schematic diagram of the dopaminergic innervation of the neocortex is depicted in Fig. 11.2. DA afferents are densest in cortical areas 24, 4, 6, and SMA, where they display a trilaminar pattern of distribution, predominating in layers I, IIIa, and V–VI [5, 54, 25, 27, 28]. In the granular prefrontal (areas 46, 9, 10, 11, 12), parietal (areas 1, 2, 3, 5, 7), temporal (areas 21, 22), and posterior cingulate (area 23) cortices, DA afferents are less dense and show a bilaminar pattern of distribution in the depth of layers I and V–VI [5, 42, 43, 27, 28, 46]. Area 17 has the lowest DA density, where the DA afferents are mostly restricted to layer I [5].

In addition to the DAergic innervation of the neocortex, the presence of dopaminergic fibers in the dorsal and ventral horns of the spinal cord has been observed by several groups [7, 8]. In the dorsal horn, DA fibers are localized in the superficial layers and in the laminae III–V and X. In ventral horn, DA fibers are found in layers VII, VIII, and laminae IX [51]. The sources of the dorsal DAergic innervation are the posterior and dorsal hypothalamic areas and the periventricular gray matter of the caudal thalamus, whereas of the ventral dopaminergic innervation is the caudal hypothalamus A11 cell group [47]. Finally, an uncrossed nigrospinal DAergic pathway has been documented by anatomical methods [15].

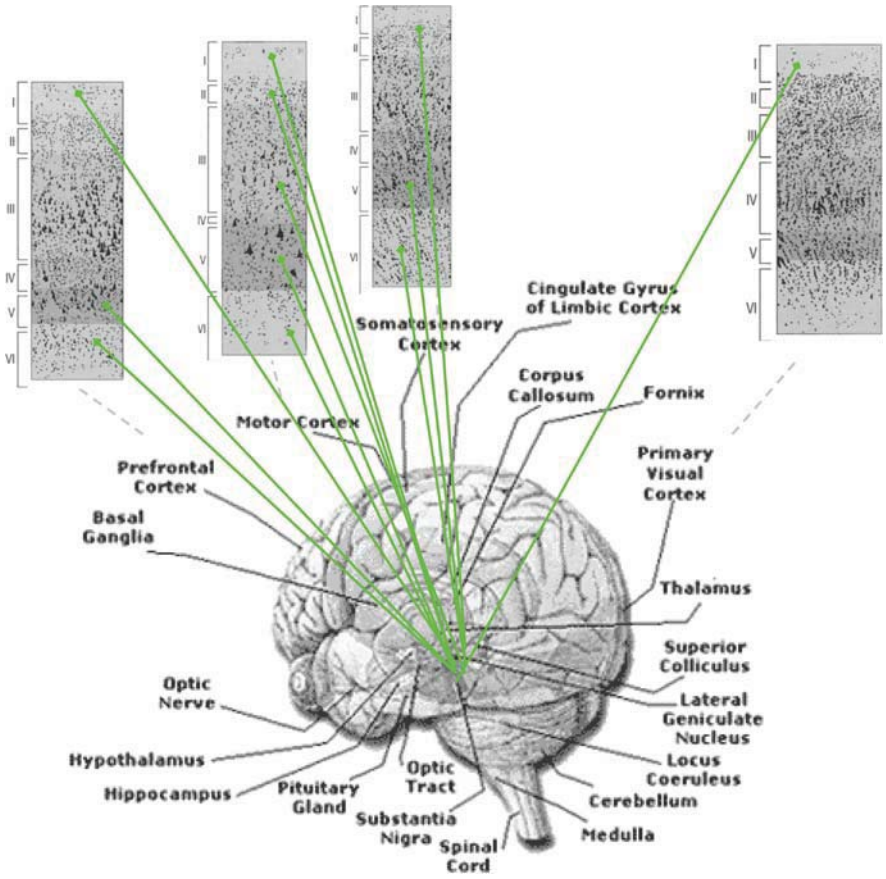

Fig. 11.2: Dopaminergic laminar innervation of the prefrontal, motor, somatosensory, and primary visual cortices from the substantia nigra pars compacta. *Diamond solid green lines*: dopamine projection from the substantia nigra.

11.5 Effects of Dopamine Depletion on Neuronal, Electromyographic, and Movement Parameters in PD Humans and MPTP Animals

The effects of dopamine depletion on neuronal, electromyographic, and movement parameters in PD humans and in MPTP-treated animals are briefly summarized below.

11.5.1 Cellular Disorganization in Cortex

Doudet and colleagues [23] trained monkeys to perform fast flexion and extension elbow movements while they recorded from their primary motor cortex before and

after 1-methyl-4-phenyl-1,2,5,6-tetrahydropyridine (MPTP) injection. A reduction in the number of reciprocally organized cells (neurons showing a reciprocal discharge pattern for flexion and extension movements; 49% in the pre-MPTP state and 18% in the post-MPTP state) and an increase in the number of unidirectional cells (cells whose activities change in only one direction; 19% in the pre-MPTP state and 50% in the post-MPTP state) without an alteration of the overall excitation were reported. It was suggested that there was a lift of inhibition from cells that are normally inhibited during movement resulting in an extra-imposed load on the limb [23].

11.5.2 Reduction of Neuronal Intensity and of Rate of Development of Neuronal Discharge in the Primary Motor Cortex

Watts and Mandir [50] examined the effects of MPTP-induced Parkinsonism on the primary motor cortex task-related neuronal activity and motor behavior of monkeys. Two monkeys were trained in the pre-MPTP state with the help of visual cues, delivered via a panel of light-emitting diodes (LEDs), to make fast, wrist flexion movements of 60. Once the animals were fully trained on the task and the M1 neuronal and EMG activities were recorded, intracarotid injection of MPTP was administered to induce a stable state of Parkinsonism. Single neuronal recordings were repeated during the experimentally induced Parkinsonian state for many months. They reported a decrease in the percentage of movement onset-related neurons and an increase in the latency between the start of M1 neuronal activity and the movement onset and in the duration of after-discharge following movement onset in the hemi-Parkinsonian state.

Similarly, Gross and colleagues [36] trained monkeys to perform a rapid elbow movement (> 30) of extension or flexion in response to an auditory signal. The unit activity of the primary motor cortical cells was recorded 500 ms before and 1,500 ms after the beginning of the auditory signal, before and after an electrolytic lesion of the substantia nigra pars compacta (SNc). They reported that the maximum discharge frequency in lesioned animals was lower than in normal animals.

Doudet and colleagues [23] observed a similar change in discharge rate of primary motor cortical cells as well as a prolongation of their total response duration. They reported that the time between the start of the alterations in the neuronal discharge and the onset of movement was increased by 20%.

11.5.3 Significant Increase in Mean Duration of Neuronal Discharge in Primary Motor Cortex Preceding and Following Onset of Movement

In the experimental paradigm described earlier, Gross and colleagues [36] observed that the latency between the onset of neuronal discharge and the beginning of fore-

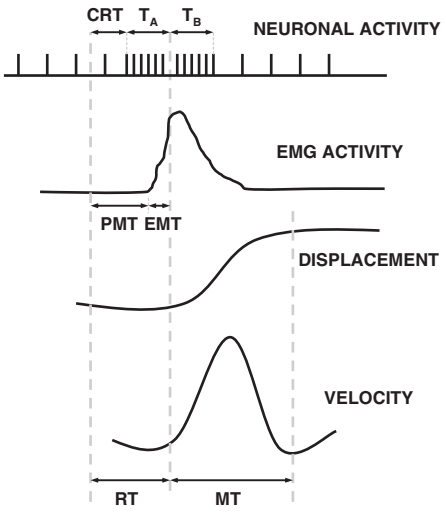

Fig. 11.3: Schematic representation of the neuronal, electromyographic, and kinematic variables. CRT: cellular reaction time; PMT: premotor time; EMT: electromechanical time; RT: reaction time; MT: movement times; T_A: time of neuronal discharge prior to movement onset; T_B: duration of neuronal discharge after movement onset.

arm displacement and the duration of the neuronal activity from the onset of movement and the time where the level of activity returned to resting levels (see Fig. 11.3 for a schematic description) were increased. Similarly, Doudet and colleagues [23] reported that the mean duration of neuronal discharge in area 4 preceding the onset of movement was slightly affected in the MPTP-treated animals, whereas the mean duration of neuronal discharge following the onset of movement was significantly increased.

11.5.4 Prolongation of Behavioral Simple Reaction Time

Benazzouz et al. [2] trained monkeys to perform a rapid elbow movement (> 40) of extension or flexion in response to an auditory signal. EMG activity was recorded with intramuscular electrodes 500 ms before and 1,500 ms after the beginning of the auditory signal, before and after an MPTP lesion of the substantia nigra pars compacta (SNc). They reported that the behavioral simple reaction time (cellular reaction time + mean duration of neuronal discharge before movement onset (TA; see Fig. 11.3) after a nigral MPTP lesion was significantly increased for both extension and flexion movements. Similarly, Doudet et al. [24, 23] and Gross et al. [36] observed a significant change in the mean values of the simple reaction time (RT)

for both flexion and extension movements in the MPTP-treated and electrolytical lesioned animals. Weiss et al. [52] investigated the kinematic organization of discrete elbow movements of different amplitudes to targets of various sizes of young, elderly, and PD subjects. The investigators reported a significant increase in the simple reaction time between young, elderly, and PD subjects over all conditions.

11.5.5 Repetitive Triphasic Pattern of Muscle Activation

Hallett and Khoshbin [37] asked healthy and Parkinson's disease (PD) patients to make rapid accurate elbow flexion movements of different angular distances (10, 20, and 40) while they recorded their EMG activities and their elbow angles with surface electrodes. They reported that healthy subjects exhibited a triphasic (agonist–antagonist–agonist) EMG pattern. However, the EMG patterns in the muscles of Parkinson's disease patients differed from those of the healthy subjects in that the bursts of EMG activity in the agonist muscle did not increase in magnitude for the larger amplitude movements. Hallett and Khoshbin [37] interpreted their results indicating that patients with PD are unable to sufficiently activate agonist muscles during movements made as quickly as possible. They showed that an apparent compensation for the decreased muscular activation was to evoke more cycles of activity to complete the movement. Doudet et al. [23] reported that in order for MPTP-treated animals to achieve the full amplitude of the required movement, additional successive bursts of lower amplitude and duration were needed.

11.5.6 Electromechanical Delay Time Is Increased

Electromechanical delay time (EMT; time between the onset of modification of agonist EMG activity and the onset of movement (OM); see Fig. 11.3) is significantly increased in MPTP-treated animals. Benazzouz et al. [2] study showed that monkeys display a significant increase in the EMD time. Doudet et al. [24, 23] in the exact same experimental paradigm observed a similar delay in EMT.

11.5.7 Depression of Rate of Development and Peak Amplitude of the First Agonist Burst of EMG Activity

Godaux and colleagues [34] conducted experiments with control and PD patients seated facing a target button. Subjects were instructed to switch off the target button when it lit, by pressing it as rapidly as possible. The activities of anterior deltoid, biceps brachii, triceps brachii, and extensor indicis muscles were recorded using sur-

face electrodes as the subjects were performing the task. Godaux et al. [34] found that the amplitudes of the peak EMG activity were reduced and the rates of development of muscle activity in both flexors and extensors were depressed in PD patients.

Corcos et al. [17] measured the maximum elbow flexor and extensor muscle strength in patients with PD during on and off anti-PD medication. Patients were tested in two maximally produced muscle isometric contractions and two flexion contractions equal to 50% of their maximal voluntary contractions. In all four conditions, the patients were seated on a table with fully supinated right forearm flexed 90° with respect to the arm and positioned vertically. The forearm was attached to a stiff steel bar and changes in torque were measured by strain gauges. EMG signals were recorded with surface electrodes. Corcos and colleagues reported a reduction in the peak torque and in the rate of change of torque.

Watts and Mandir [50] trained PD patients and age-matched controls to perform a rapid, wrist flexion task. Their hands were hidden from their view. Visual cues were used to instruct the subjects where and when to move. The subjects were advised to move as quickly and as accurately as possible once they were given the go-signal. Their flexor and extensor electromyographic (EMG) activities were recorded using surface electrodes during the trials. They noted decreased average amplitude of EMG activity for the patients with Parkinson's disease. Doudet et al. [24, 23] reported that the rate of development and peak amplitude of the first agonist burst of EMG activity were depressed. Similarly, Hallett and Khoshbin [37] observed, in patients with Parkinson's disease, there was a similar reduction in the activity of the first agonist burst as if it has reached a ceiling.

11.5.8 Movement Time Is Significantly Increased

Rand et al. [45] trained PD patients and age-matched controls to make rapid arm movements with or without accuracy constraints. Subjects were seated in front of a horizontal digitizer and held a stylus. The subject was required to move the stylus from a home position to a target position after an auditory signal. In the spatial accuracy condition, the subjects were required to move the stylus to the defined target and stop on it, whereas in the *n*-spatial accuracy condition, the subjects were asked to move toward the target without stopping precisely on it. The subjects were asked to make their movements as fast and as accurate as possible. Rand et al. [45] reported that the movements of patients were slower than those of the controls in both the acceleration phase and the deceleration phase. The prolonged deceleration phase for the patients was more pronounced in the target condition. In addition, the kinematics of PD patients were abnormal, characterized by a higher number of acceleration zero crossings indicating that their movements were segmented and that the first zero crossing occurred much earlier in the movement. Weiss et al. [52] trained and tested young, elderly, and PD subjects in making discrete elbow movements with varying amplitudes to targets of varying sizes. They reported that

both the acceleration and the deceleration times were increased. Doudet et al. [24, 23] and Benazzouz et al. [2] reported a 25–30% increase in movement duration in monkeys treated with MPTP compared to normal monkeys. Watts and Mandir [50] showed that both MPTP-treated animals and Parkinson's disease patients take longer time to complete the required movements.

11.5.9 Reduction of Peak Velocity

In the experimental study described earlier, one of Godaux et al. [34] findings was a profound decrease in the peak velocity of movement of PD patients. Camarata et al. [13] reported that in the MPTP-treated animals, the velocity profiles appeared less smooth and the amplitude of the velocity profile decreased and delayed in time at most distances and directions tested. Weiss et al. [52] observed a similar decrease in the peak velocity of movement of PD patients. Further, Benazzouz et al. [2] and Doudet et al. [24, 23] after treating monkeys with MPTP found a significant decrease in the amplitude of their velocity profiles. Rand et al. [45] reported a significant reduction of the peak velocity in both accuracy and no-accuracy movement conditions.

11.5.10 Reduction of Peak Force and Rate of Force Production

Stelmach et al. [48] examined the preparation and the production of isometric force in Parkinson's disease. PD patients, elderly, and young subjects were asked to generate a percentage of their maximum force levels. PD patients showed a similar progression of force variability and dispersion of peak forces to that of control subjects. Force production impairments were seen at the within-trial level. PD patients were substantially slower in initiating a force production and their peak forces were reduced.

11.5.11 Movement Variability

Camarata et al. [13] trained monkeys to make two-joint movements on a horizontal plane by moving a manipulandum in six different directions (30, 90, 150, 210, 270, and 330) at five distances from a central start box. Velocity and acceleration profiles were calculated for both pre- and post-MPTP states. They reported a marked variability in the onset, peak velocity, and time course of the velocity profile of MPTP-treated monkeys. Similarly, Stelmach et al. [48] reported variability in the force profile of Parkinson's disease patients.

11.6 The Extended VITE–FLETE Models with Dopamine

Figure 11.4 depicts the extended VITE–FLETE with dopamine model of voluntary movement preparation and execution in Parkinson's disease. In the previous chapter, the temporal development of the model without dopamine was discussed. The model under normal conditions successfully predicted the origin of the triphasic pattern of muscle activation and its neural substrates. In this chapter and although a much larger set of experimental data has been briefly described in the previous section, I will describe how the triphasic pattern and its neural and EMG substrates change when dopamine is depleted in basal ganglia, cortex, and spinal cord. Detailed descriptions of the model and its complete mathematical formalism

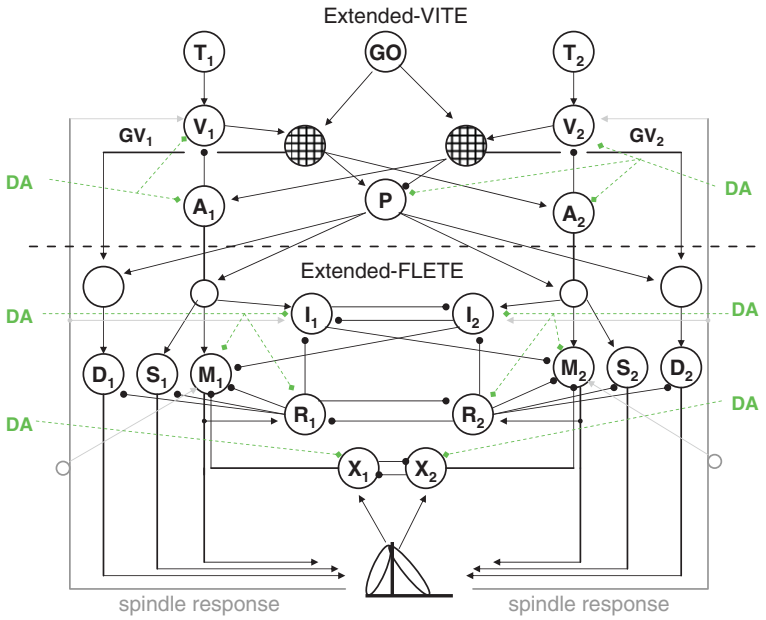

Fig. 11.4: Extended VITE–FLETE models with dopamine (DA). *Top*: DA–VITE model for variable-speed trajectory generation. *Bottom*: DA–FLETE model of the opponent processing spinomuscular system. *Arrow lines*: excitatory projections; *solid dot lines*: inhibitory projections; *diamond-dotted green lines*: dopamine modulation; *dotted arrow lines*: feedback pathways from sensors embedded in muscles. *GO*: basal ganglia output signal; *P*: bidirectional co-contractive signal; *T*: target position command; *V*: DV activity; *GV*: DVV activity; *A*: current position command; *M*: alpha motoneuronal (MN) activity; *R*: renshaw cell activity; *X, Y, Z*: spinal inhibitory interneuron (IN) activities; I_a: spinal type a inhibitory IN activity; *S*: static gamma MN activity; *D*: dynamic gamma MN activity; *1,2*: antagonist cell pair.

can be found in Cutsuridis and Perantonis [21] and Cutsuridis [18, 19, 20]. As in the extended model without dopamine (see previous chapter), the GO signal was defined by

$$G(t) = G_0(t-\tau_i)^2 u[t-\tau_i]/(\beta+\gamma(t-\tau_i)^2), \tag{11.1}$$

where G_0 amplifies the G_0 signal, i is the onset time of the ith volitional command, β and γ are free parameters, and $u[t]$ is a step function that jumps from 0 to 1 to initiate movement. The difference vector (DV) with dopamine was described by

$$\frac{dV_i}{dt} = 30(-V_i + T_i - \mathrm{DA}_1 A_i + \mathrm{DA}_1 a_w(W_i(t-\tau) - W_j(t-\tau))), \tag{11.2}$$

where T_i is the target position command, A_i is the current limb position command, a_w is the gain of the spindle feedback, $W_{i,j}$ are the spindle feedback signals from the antagonist muscles, and DA_1 is the modulatory effect of dopamine on area 4's PPV inputs to DV cell activity. Dopamine's values ranged from 0 (lesioned) to 1 (normal). The desired velocity vector (DVV) with dopamine which represented area's 4 reciprocally activated cell activity was defined by

$$u_i = \left[G(\mathrm{DA}_2 V_i - \mathrm{DA}_3 V_j + \frac{B_u}{\mathrm{DA}_4}\right]^+, \tag{11.3}$$

where i, j designate opponent neural commands, B_u is the baseline activity of the phasic-MT area 4 cell activity, and DA_2, DA_3 are the modulatory effects of dopamine on DV inputs to DVV cell activity and DA_4 is the effect of dopamine on DVV baseline activity. The reader can notice that parameter DA_1 modulates the PPV input to area's 5 phasic (DV) cell activity (Equation 11.2), whereas parameters DA_2, DA_3, and DA_4 modulate the DV inputs to DVV and P cell activity (area's 4 reciprocal and bidirectional activities) and to DVV baseline activity (Equations 11.3 and 11.4), respectively. This is, as we explained in a previous section, because DA afferents are densest in area 4 than they are in area 5. So, the effect of DA depletion would be stronger in area 4 than in area 5. Also, the DV flexion (V_i) cell is modulated by a different DA parameter DA_2) from the DV extension (V_j) cell (DA_3). The latter is supported by the experimental findings of Doudet and colleagues [23] (for comparison see Figs. 11.4 and 11.5, where the firing intensity of the flexion cells is affected (reduced) more than the firing intensity of the extension cells). The co-contractive vector (P) with dopamine which was represented by area's 4 bidirectional neuronal activity was given by

$$u_i = \left[G(\mathrm{DA}_2 V_i - \mathrm{DA}_3 V_j + \frac{B_P}{\mathrm{DA}_4}\right]^+, \tag{11.4}$$

whereas the present position vector (PPV) dynamics was defined by

$$\frac{dA_i}{dt} = G[DA_2.V_i]^+ - G[DA_3.V_j]^+. \tag{11.5}$$

The renshaw population cell activity with dopamine was modeled by

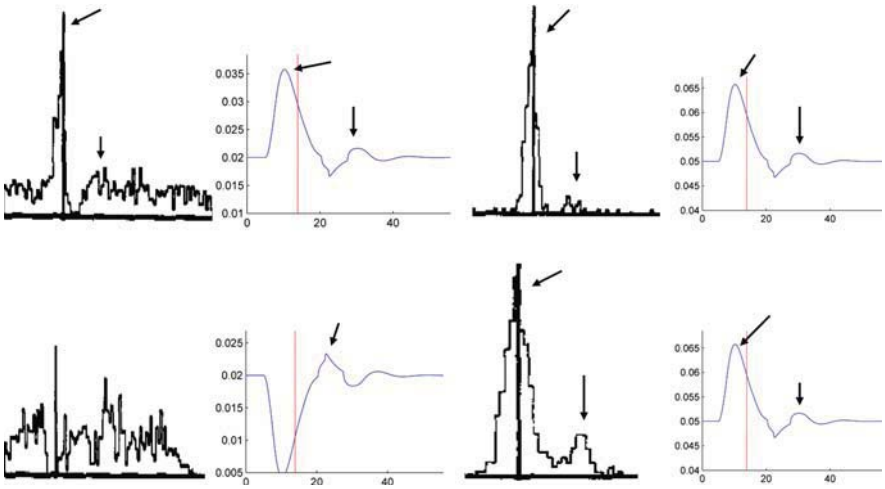

Fig. 11.5: Comparison of peristimulus time histograms (PSTH) of reciprocally organized neurons (column 1; reproduced with permission from Doudet et al. [23, Fig. 4A, p. 182], Copyright Springer-Verlag) in area 4, simulated area's 4 reciprocally organized phasic (DVV) cell activities (column 2), PSTH of area's 4 bidirectional neurons (column 3; reproduced with permission from [23, Fig. 4A, p. 182], Copyright Springer-Verlag) and simulated area's 4 co-contractive (P) cells activities (column 4) for a flexion (row 1) and extension (row 2) movements in normal monkey. The *vertical bars* indicate the onset of movement. Note a clear triphasic AG1-ANT1-AG2 pattern marked with *arrows* is evident in PSTH of reciprocally and bidirectionally organized neurons. The same triphasic pattern is evident in simulated DVV cell activities. The second peak in simulated activities marked with an arrow arises from the spindle feedback input to area's 5 DV activity.

$$\frac{dR_i}{dt} = \phi(\lambda B_i - R_i)\mathrm{DA}_5 z_i \max(M_i,0) - \mathrm{DA}_6 R_i(1.5+\max(R_j,0)), \tag{11.6}$$

whereas the $\alpha-$MN population activity with dopamine was described by

$$\begin{aligned}\frac{M_i}{dt} = \phi\ & (\lambda B_i - M_i)\mathrm{DA}_7(A_i+P+\chi E_i) - (M_i+2)\mathrm{DA}_8(1+\Omega\max(R_i,0) \\ & + \rho\max(X_i,0)+\max(I_j,0))\end{aligned} \tag{11.7}$$

where X_i is the type I_b interneuron (I_bIN) force feedback, E_i is the stretch feedback, and I_j is the type I_a interneuron. The type I_a interneuron (I_aIN) population activity with dopamine was defined as

$$\begin{aligned}\frac{dI_i}{dt} = \phi\ & (15-I_i)\mathrm{DA}_9(A_i+P+\chi E_i) - \mathrm{DA}_{10} I_i(1+\Omega\max(R_i,0) \\ & + \max(I_j,0)).\end{aligned} \tag{11.8}$$

The I_bIN population activity with dopamine was given by

$$\frac{dX_i}{dt} = \phi A_{11}(15 - X_i)F_i - X_i \mathrm{DA}_{11}(0.8 + 2.2\max(X_j, 0)), \tag{11.9}$$

where F_i is the feedback activity of force-sensitive Golgi tendon organs.

11.7 Simulated Effects of Dopamine Depletion on the Cortical Neural Activities

Figures 11.5 and 11.6 show qualitative comparisons of experimental and simulated neuronal discharges of reciprocal and bidirectional neurons in normal and dopamine-depleted conditions, respectively. It is clearly evident an overall reduction of firing intensity [23, 36], a reduced rate of change of neuronal discharge [23, 36], a disorganization of neuronal activity (neuronal direction specificity is markedly reduced) [23], and an increase in baseline activity (in the normal case the baseline activity was 0.05, whereas in dopamine depleted the baseline activity increased to 0.07) [23]. Figure 11.8 shows a qualitative comparison of abnormal cellular responses of GPi neurons to striatal stimulation in MPTP-treated monkeys (column 1 of Fig. 11.8) and simulated GPi neuronal responses (column 2 of Figure 11.8).

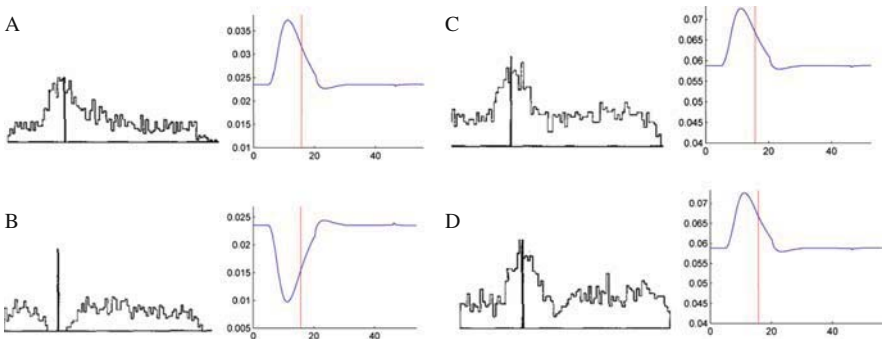

Fig. 11.6: Comparison of peristimulus time histograms (PSTH) of reciprocally organized neurons (column 1; reproduced with permission from [23, Fig. 4A, p. 182], Copyright Springer-Verlag) in area 4, simulated area's 4 reciprocally organized phasic (DVV) cell activities (column 2), PSTH of area's 4 bidirectional neurons (column 3; reproduced with permission from [23], Fig. 4A, p. 182, Copyright Springer-Verlag) and simulated area's 4 co-contractive (P) cells activities (column 4) for a flexion (**A** and **C**) and extension (**B** and **D**) movements in MPTP-treated monkey. The *vertical bars* indicate the onset of movement. Note that the triphasic pattern is disrupted: Peak AG1 and AG2 bursts have decreased, and ANT pause is shortened.

In their study, Tremblay and colleagues [49] observed an abnormal oscillatory GPi response, but failed to offer a functional role for it oscillatory responses. We propose that such GPi oscillatory responses (repetitive GO signal), comprising of at least two inhibitory–excitatory sequences, gate (multiply) the DV signal and generate repetitive volitional motor commands (DVV signals; not shown), which in turn generate repetitive agonist–antagonist muscle bursts (see row 2, column 3 of Figure 11.8) needed sometimes by PD patients to complete the full amplitude of the movement.

11.8 Simulated Effects of Dopamine Depletion on EMG Activities

As mentioned in the previous chapter, single ballistic movements at a joint in normal individuals are made with a single biphasic (sometimes triphasic) pattern of EMG activity in agonist and antagonist muscles [39, 4, 9, 10, 11, 35, 29, 30, 31, 53, 38]. In PD patients, the size of the first agonist burst is reduced. Up to a certain size, movements might be performed by a single agonist-antagonist pattern of muscle activation [26], but there are times that movements would require additional bursts of EMG activity [37, 2, 23] in order for the limb to reach the target. The extended DA–VITE–FLETE model has offered a plausible hypothesis of why PD EMG agonist burst activity is reduced and why sometimes multiple bursts of AG-ANT-

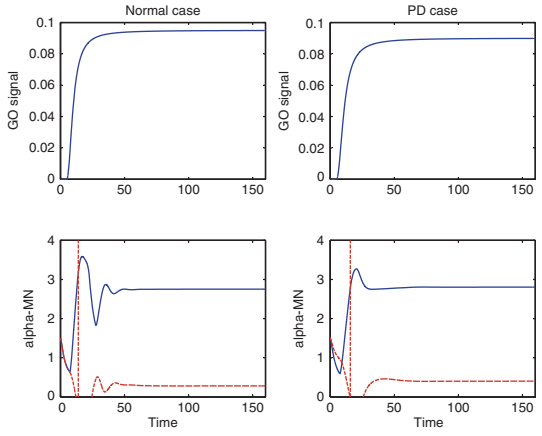

Fig. 11.7: Comparison of simulated GO signals (row 1) and α-MN activities (row 2) in normal (column 1) and dopamine-depleted (column 2) conditions. (Row 2) *Blue solid curve*: agonist α-MN activity; *Red-dashed curve*: antagonist α-MN activity. Note in PD case, the triphasic pattern is disrupted and it is replaced by a biphasic pattern of muscle activation. Also, the peaks of agonist and antagonist bursts are decreased.

AG are needed to complete the movement. According to the model, disruptions of the GO signal and dopamine depletion in the cortex and spinal cord disrupt the reciprocal organization of M1 neurons, reduce their activity, increase their rate of change, and hence result in the downscaling of the size of the first agonist burst and in the increase of its rate of change. So, in order for the subject to complete the movement and reach the target, additional EMG bursts are required. Figure 11.7 shows a qualitative comparison of the normal (column 1) and dopamine-depleted (column 2) simulated alpha motoneuronal (MN) activities of the agonist and antagonist muscles. A significant reduction in the peak agonist and antagonist amplitude as well as of their rate of development is evident [50, 23, 37, 17]. In contrast to some PD studies [2, 24, 40], a single and non co-contractive agonist-antagonist pattern of muscle activation is observed (column 2 of figure 11.7). Figure 11.8 shows a qualitative comparison of the experimental (column 1) and simulated (column 2) GPi discharge patterns (GO signal) and α-MN activity (column 3) in normal (row 1) and PD (row 2) large amplitude movement conditions. An abnormal oscillatory GO signal and DA depletion in the cortex and spinal cord result in a repetitive biphasic pattern of muscle activation (indicated by the arrows) necessary to complete the movement [37]. In the model, the generation of such repetitive biphasic pattern of

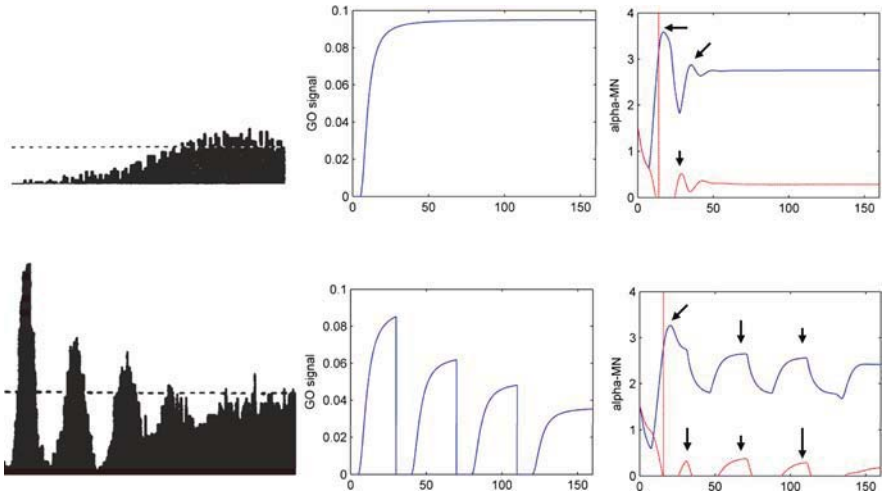

Fig. 11.8: Comparison of the experimental GPi PSTH (column 1), GO signals (column 2), and α-MN activities (column 3) in normal (row 1) and dopamine-depleted (row 2) conditions. (*Column 3, rows 1 and 2*) *Blue-colored solid curve*: agonist α-MN unit; *Red-colored dashed curve*: antagonist α-MN unit. Note in dopamine-depleted case the α-MN activity is disrupted and replaced by repetitive and co-contractive agonist–antagonist bursts (*row 2, column 3*). (*Column 1, row 1*) GPi PSTH in intact monkey reproduced with permission from Tremblay et al. [49, Fig. 4, p. 6], Copyright Elsevier. (*Column1, row 2*) GPi PSTH in MPTP monkey reproduced with permission from [49, Fig. 2, p. 23], Copyright Elsevier.

muscle activation is the result of the gating of the DV signal by multiple inhibition–excitation sequences of abnormal GO signal for the generation of multiple volitional motor cortical commands sent down to the spinal cord for the completion of the movement.

11.9 Conclusion

This chapter has focused on how the smooth organization of voluntary movement observed in normal individuals is disrupted in Parkinson's disease. The neural network model of voluntary movement preparation and execution presented in the previous chapter was extended by studying the effects of dopamine depletion in the output of the basal ganglia and in key neuronal types in cortex and spinal cord. The resulting extended DA–VITE–FLETE model offered an integrative perspective on corticospinal control of Parkinsonian voluntary movement. The model accounted for some of the known empirical signatures of Parkinsonian willful action:

- Cellular disorganization in cortex
- Increases in neuronal baseline activity
- Reduction of firing intensity and firing rate of cells in primary motor cortex
- Abnormal oscillatory GPi response
- Disinhibition of reciprocally tuned cells
- Repetitive bursts of muscle activation
- Reduction in the size and rate of development of the first agonist burst of EMG activity
- Repetitive triphasic pattern of muscle activation
- Non co-contraction of antagonist MN units in small amplitude movements
- Co-contraction of antagonist MN units in large amplitude movements

The interested reader should refer to the modeling studies of Cutsuridis and Perantonis [21] and Cutsuridis [18, 19, 20], where additional empirical signatures of PD kinematics have been successfully simulated:

- Increased duration of neuronal discharge in area 4 preceding and following onset of movement
- Prolongation of premotor and electromechanical delay times
- Asymmetric increase in the time-to-peak and deceleration time
- Decrease in the peak value of the velocity trace
- Increase in movement duration
- Movement variability

All these results provided sufficient evidence to support the main hypothesis of the model, which stated that "elimination of DA modulation from the SNc disrupts, via several pathways, the buildup of the pattern of movement-related responses in the primary motor and parietal cortex, and results in a loss of directional specificity of reciprocal and bidirectional cells in the motor cortex as well as in a reduction in their activities and their rates of change. These changes result in delays in recruiting

the appropriate level of muscle force sufficiently fast and in an inappropriate scaling of the dynamic muscle force to the movement parameters. A repetitive triphasic pattern of muscle activation is sometimes needed to complete the movement. All of these result in an increase of mean reaction time and a slowness of movement" [21].

References

1. Albin, R., Young, A., Penney, J. The functional anatomy of basal ganglia disorders. Trends Neurosci **12**, 366–375 (1989)
2. Benazzouz, A., Gross, C., Dupont, J., Bioulac, B. MPTP induced hemiparkinsonism in monkeys: Behavioral, mechanographic, electromyographic and immunohistochemical studies. Exp Brain Res **90**, 116–120 (1992)
3. Benecke, R., Rothwell, J., Dick, J. Performance of simultaneous movements in patients with Parkinson's disease. Brain **109**, 739–757 (1986)
4. Berardelli, A., Dick, J., Rothwell, J., Day, B., Marsden, C. Scaling of the size of the first agonist EMG burst during rapid wrist movements in patients with Parkinson's disease. J Neurol Neurosurg Psych **49**, 1273–1279 (1986)
5. Berger, B., Trottier, S., Verney, C., Gaspar, P., Alvarez, C. Regional and laminar distribution of dopamine and serotonin innervation in the macaque cerebral cortex: A radioautographic study. J Comp Neurol **273**, 99–119 (1988)
6. Bjorklund, A., Lindvall, O. Dopamine containing systems in the CNS. Classical Transmitters in the CNS: Part 1, Handbook of Chemical Neuroanatomy, Vol. 2, pp. 55–121. Elsevier, Amsterdam (1984)
7. Bjorklund, A., Skagerberg, G. Evidence of a major spinal cord projection from the diencephalic A11 dopamine cell group in the rat using transmitter-specific fluoroscence retrograde tracing. Brain Res **177**, 170–175 (1979)
8. Blessing, W., Chalmers, J. Direct projection of catecholamine (presumably dopamine)-containing neurons from the hypothalamus to spinal cord. Neurosci Lett **11**, 35–40 (1979)
9. Brown, S., Cooke, J. Initial agonist burst duration depends on movement amplitude. Exp Brain Res **55**, 523–527 (1984)
10. Brown, S., Cooke, J. Movement related phasic muscle activation I. Relations with temporal profile of movement. J Neurophys **63**(3), 455–464 (1990)
11. Brown, S., Cooke, J. Movement related phasicmuscle activation II. Generation and functional role of the triphasic pattern. J Neurophysiol **63**(3), 465–472 (1990)
12. Burns, R., Chiueh, C., Markey, S., Ebert, M., Jacobowitz, D., Kopin, I. A primate model of parkinsonism: Selective destruction of dopaminergic neurons in the pars compacta of the substantia nigra by n-methyl-4-phenyl-1,2,3,6-tetrahydropyridine. Proc Natl Acad Sci USA **80**, 4546–4550 (1983)
13. Camarata, P., Parker, R., Park, S., Haines, S., Turner, D., Chae, H., Ebner, T. Effects of MPTP induced hemiparkinsonism on the kinematics of a twodimensional, multi-joint arm movement in the rhesus monkey. Neuroscience **48**(3), 607–619 (1992)
14. Carlsson, A., Lindquist, M., Magnusson, T. 3,4-dihydroxyphenylalanine and 5-hydroxytryptophan as reserpine antagonists. Nature **180**, 1200 (1957)
15. Commissiong, J., Gentleman, S., Neff, N. Spinal cord dopaminergic neurons: Evidence for an uncrossed nigrostriatal pathway. Neuropharmacology **18**, 565–568 (1979)
16. Connor, N., Abbs, J. Task-dependent variations in parkinsonianmotor impairments. Brain **114**, 321–332 (1991)
17. Corcos, D., Jaric, S., Gottlieb, G. Electromyographic analysis of performance enhancement. Advances in Motor Learning and Control. Human Kinetics, Champaign, IL (1996)
18. Cutsuridis, V. Neural model of dopaminergic control of arm movements in Parkinson's disease Bradykinesia. Artificial Neural Networks, *LNCS*, Vol. 4131, pp. 583–591. Springer-Verlag, Berlin (2006)

19. Cutsuridis, V. Biologically inspired neural architectures of voluntary movement in normal and disordered states of the brain. Ph.D. Thesis (2006). Unpublished Ph.D. dissertation. http://www.cs.stir.ac.uk/ vcu/papers/PhD.pdf
20. Cutsuridis, V. Does reduced spinal reciprocal inhibition lead to co-contraction of antagonist motor units? a modeling study. Int J Neural Syst **17**(4), 319–327 (2007)
21. Cutsuridis, V., Perantonis, S. A neural model of Parkinson's disease bradykinesia. Neural Netw **19**(4), 354–374 (2006)
22. Davis, G., Williams, A., Markey, S., Ebert, M., Calne, E., Reichert, C., Kopin, I. Chronic parkinsonism secondary to intravenous injection of meperidine analogues. Psychiatr Res **1**, 249–254 (1979)
23. Doudet, D., Gross, C., Arluison, M., Bioulac, B. Modifications of precentral cortex discharge and EMG activity in monkeys with MPTP induced lesions of DA nigral lesions. Exp Brain Res **80**, 177–188 (1990)
24. Doudet, D., Gross, C., Lebrun-Grandie, P., Bioulac, B. MPTP primate model of Parkinson's disease: A mechanographic and electromyographic study. Brain Res **335**, 194–199 (1985)
25. Elsworth, J., Deutch, A., Redmond, D., Sladek, J., Roth, R. MPTP reduces dopamine and norepinephrine concentrations in the supplementary motor area and cingulate cortex of the primate. Neurosci Lett **114**, 316–322 (1990)
26. Flowers, K. Visual "closed-loop" and "open-loop" characteristics of voluntary movement in patients with parkinsonism and intention tremor. Brain **99**(2), 269–310 (1976)
27. Gaspar, P., Duyckaerts, C., Alvarez, C., Javoy-Agid, F., Berger, B. Alterations of dopaminergic and noradrenergic innervations in motor cortex in Parkinson's disease. Ann Neurol **30**, 365–374 (1991)
28. Gaspar, P., Stepniewska, I., Kaas, J. Topography and collateralization of the dopaminergic projections to motor and lateral prefrontal cortex in owl monkeys. J Comp Neurol **325**, 1–21 (1992)
29. Ghez, C., Gordon, J. Trajectory control in targeted force impulses. I. Role in opposing muscles. Exp Brain Res **67**, 225–240 (1987)
30. Ghez, C., Gordon, J. Trajectory control in targeted force impulses. II. Pulse height control. Exp Brain Res **67**, 241–252 (1987)
31. Ghez, C., Gordon, J. Trajectory control in targeted force impulses. III. Compensatory adjustments for initial errors. Exp Brain Res **67**, 253–269 (1987)
32. Gibb, W., Lees, A., Jenner, P., Marsden, C. MPTP: Effects of MPTP in the mid-brain of marmoset. A Neurotoxin Producing A Parkinsonian Syndrome, pp. 607–614. Academic Press, New York (1986)
33. Gibberd, F. The management of Parkinson's disease. Practitioner **230**, 139–146 (1986)
34. Godaux, E., Koulischer, D., Jacquy, J. Parkinsonian bradykinesia is due to depression in the rate of rise of muscle activity. Ann Neurol **31**(1), 93–100 (1992)
35. Gottlieb, G., Latash, M., Corcos, D., Liubinskas, A., Agarwal, G. Organizing principle for single joint movements: I. agonist-antagonist interactions. J Neurophys **13**(6), 1417–1427 (1992)
36. Gross, C., Feger, J., Seal, J., Haramburu, P., Bioulac, B. Neuronal activity of area 4 and movement parameters recorded in trained monkeys after unilateral lesion of the substantia nigra. Exp Brain Res Suppl. **7**, 181–193 (1983)
37. Hallett, M., Khoshbin, S. A physiological mechanism of bradykinesia. Brain **103**, 301–314 (1980)
38. Hallett, M., Marsden, G. Ballistic flexion movements of the human thumb. J Physiol **294**, 33–50 (1979)
39. Hallett, M., Shahani, B., Young, R. EMG analysis of stereotyped voluntary movements. J Neurol Neurosurg Psychiatr **38**, 1154–62 (1975)
40. Hayashi, A., Kagamihara, Y., Nakajima, Y., Narabayashi, H., Okuma, Y., Tanaka, R. Disorder in reciprocal innervation upon initiation of voluntary movement in patients with Parkinson's disease. Exp Brain Res **70**, 437–440 (1988)
41. Lazarus, J., Stelmach, G. Inter-limb coordination in Parkinson's disease. Mov Disord 7, 159–170 (1992)

42. Lewis, D., Morrison, J., Goldstein, M. Brainstem dopaminergic neurons project to monkey parietal cortex. Neurosci Lett **86**, 11–16 (1988)
43. Lidow, M., Goldman-Rakic, P., Gallager, D., Geschwind, D., Rakic, P. Distribution of major neurotransmitter receptors in the motor and somatosensory cortex of the rhesus monkey. Neuroscience **32**(3), 609–627 (1989)
44. Pifl, C., Bertel, O., Schingnitz, G., Hornykiewitz, O. Extrastriatal dopamine in symptomatic and asymptotic rhesus monkey treated with 1-methyl-4-phenyl-1,2,3,6-tetrahydropyridine (MPTP). Neurochem Int **17**, 263–270 (1990)
45. Rand, M., Stelmach, G., Bloedel, J. Movement accuracy constraints in Parkinson's disease patients. Neuropsychologia **38**, 203–212 (2000)
46. Scatton, B., Javoy-Agid, F., Rouquier, L., Dubois, B., Agid, Y. Reduction of cortical dopamine, noradrenaline, serotonin and their metabolites in Parkinson's disease. Brain Res **275**, 321–328 (1983)
47. Shirouzou, M., Anraku, T., Iwashita, Y., Yoshida, M. A new dopaminergic terminal plexus in the ventral horn of the rat spinal cord. Immunohistochemical studies at the light and the electron microscopic levels. Experientia **46**, 201–204 (1990)
48. Stelmach, G., Teasdale, N., Phillips, J., Worringham, C. Force production characteristics in parkinson's disease. Exp Brain Res **76**, 165–172 (1989)
49. Tremblay, L., Filion, M., Bedard, P. Responses of pallidal neurons to striatal stimulation in monkeys with MPTP-induced parkinsonism. Brain Res **498**(1), 17–33 (1989)
50. Watts, R., Mandir, A. The role of motor cortex in the pathophysiology of voluntary movement deficits associated with parkinsonism. Neurol Clin **10**(2), 451–469 (1992)
51. Weil-Fugazza, J., Godefroy, F. Dorsal and ventral dopaminergic innervation of the spinal cord: Functional implications. Brain Res Bull **30**, 319–324 (1993)
52. Weiss, P., Stelmach, G., Adler, C., Waterman, C. Parkinsonian arm movements as altered by task difficulty. Parkinsonism Relat Disord **2**(4), 215–223 (1996)
53. Wierzbicka,M.,Wiegner, A., Shahani, B. Role of agonist and antagonistmuscles in fast arm movements. Exp Brain Res **63**, 331–340 (1986)
54. Williams, S., Goldman-Rakic, P. Widespread origin of the primate mesofrontal dopamine system. Cereb Cortex **8**, 321–345 (1998)